

CAT: Coordinating Anatomical-Textual Prompts for Multi-Organ and Tumor Segmentation

Zhongzhen Huang^{1,2}, Yankai Jiang², Rongzhao Zhang²,
Shaoting Zhang^{1,2}, Xiaofan Zhang^{1,2}

¹Qing Yuan Research Institute, Shanghai Jiao Tong University ²Shanghai AI Laboratory


{huangzhongzhen, xiaofan.zhang}@sjtu.edu.cn,
{jiangyankai, zhangrongzhao, zhangshaoting}@pjlab.org.cn

Abstract

Existing promptable segmentation methods in the medical imaging field primarily consider either textual or visual prompts to segment relevant objects, yet they often fall short when addressing anomalies in medical images, like tumors, which may vary greatly in shape, size, and appearance. Recognizing the complexity of medical scenarios and the limitations of textual or visual prompts, we propose a novel dual-prompt schema that leverages the complementary strengths of visual and textual prompts for segmenting various organs and tumors. Specifically, we introduce **CAT**, an innovative model that Coordinates Anatomical prompts derived from 3D cropped images with Textual prompts enriched by medical domain knowledge. The model architecture adopts a general query-based design, where prompt queries facilitate segmentation queries for mask prediction. To synergize two types of prompts within a unified framework, we implement a ShareRefiner, which refines both segmentation and prompt queries while disentangling the two types of prompts. Trained on a consortium of 10 public CT datasets, **CAT** demonstrates superior performance in multiple segmentation tasks. Further validation on a specialized in-house dataset reveals the remarkable capacity of segmenting tumors across multiple cancer stages. This approach confirms that coordinating multimodal prompts is a promising avenue for addressing complex scenarios in the medical domain. Codes are available at <https://github.com/zongzi3zz/CAT>.

1 Introduction

Advanced prompt engineering [1, 2] has augmented large language models [3–5] with emerging capabilities. However, these paradigms have not yet been successfully applied to vision tasks, primarily due to the ever-changing and unpredictable natures of computer vision [6, 7]. This is particularly evident in medical domains, where variations in imaging protocols, noise/artifacts, and patient-specific pathologies pose significant challenges [8–10]. To tackle these challenges, there have been some efforts within the community to develop promptable models for segmenting objects in medical images: 1) One type of such effort focuses on textual-prompted models [11–13], which show profound competencies in segmenting a specific organ or tumor referenced by arbitrary text phrases. These approaches involve distilling knowledge from language models like CLIP [14] or BERT [15] to facilitate the alignment between visual and textual representations; 2) Another direction in promptable segmentation research aims to visual-prompted models [16–21], which rely on visual examples or visual landmarks (e.g., boxes and points). Recently, the trend toward visual-prompted segmentation models in the medical domain mainly focuses on fine-tuning SAM [22] with lightweight, plug-and-play adapters or modifying SAM into 3D-based architecture.

 Corresponding authors.

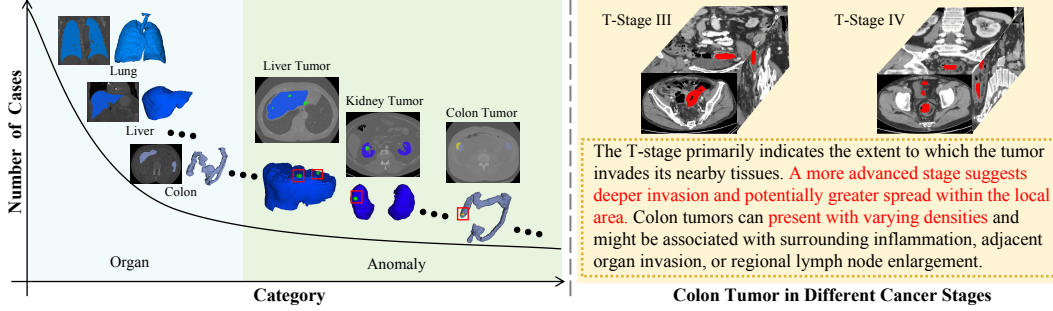


Figure 1: Left: Long-tailed curve of the category and the number of available cases that can be obtained in the medical field. Right: Tumors in different cancer staging with diverse shapes and sizes.

Despite the promising advancements brought by the prompt-enhanced segmentation paradigm, those segmentation models still face significant limitations. As illustrated in the left part of Figure 1, the distribution of medical datasets often follows a long-tail pattern, where an increase in the diversity of detectable anomalies corresponds with a sharp decline in the number of available cases. Textual-prompted methods utilize textual representations from referred text phrases to guide the segmentation process, requiring alignment between visual and textual representations. Although descriptive texts can cover intricate and rare anomalies with domain knowledge, data scarcity due to long-tailed distribution hinders the effective learning of alignments between textual and visual representations. This issue is particularly significant in the medical domain, where numerous corner cases (e.g., tumors with variations in shape, size, density distribution, and blurring boundaries) need to be addressed. Conversely, visual prompts are not constrained to the need for cross-modal alignment, providing a more intuitive and direct method to enhance the segmentation process. Nonetheless, visual prompts fail to convey the general concept of each object, leading to a performance drop when confronted with various scenarios in medical domains, especially for tumors. For instance, colon tumors range from different cancer stages [23] and have significant inter- and intra-patient in tumor sizes and shapes, as shown in the right part of Figure 1. Moreover, tumors at the same stage can exhibit varying densities. Given the inherent diversity in tumors, there is a necessity to provide comprehensive knowledge of each tumor type via textual descriptions.

In this work, we strive to develop a promptable segmentation model that utilizes the strengths of both visual and textual prompts without human interaction, aiming at a fully automatic model for medical professionals. We propose a new dual-perspective prompting scheme. On the one hand, we directly employ the cropped volumes derived from the anatomical structure as our visual prompts. We refer to such prompts as anatomical prompts, intending to represent target objects in a more intuitive and visually coherent manner. On the other hand, we enhance the textual prompts with more comprehensive knowledge. With the proposed prompting scheme, we introduce *CAT*, a model towards comprehensive segmentation that harnesses a dual-prompting mechanism to Coordinate Anatomical and Textual prompts.

CAT follows the general query-based design with two extra parallel encoders dedicated to processing anatomical and textual prompts into prompt queries. Inspired by previous segmentation models [24–27], we adopt query embeddings to perform mask predictions. A ShareRefiner is utilized to refine segmentation queries and prompt queries by attending them to image features from the backbone. We employ two distinct feature assignment strategies for prompt queries, ensuring that these prompt queries are disentangled for more versatile representations. Following the refinement process, PromptRefer updates segmentation queries by integrating both types of prompt queries. The mask prediction module then generates binary masks by performing a simple dot-product of segmentation query embeddings with the pixel embedding map obtained from the backbone. To further facilitate the coordination, we augment *CAT* with cross-modal alignment between anatomical and textual prompts. By training on an assembly of 10 public CT datasets in the abdomen, *CAT* demonstrates strong segmentation capabilities on these datasets and achieves remarkable results on an in-house dataset encompassing four cancer stages. Further ablation analysis shows that anatomical and textual prompts serve complementary roles. To summarize, our contributions are threefold:

- We design a new prompting scheme that utilizes both complementary strengths of anatomical prompts and textual prompts for medical image segmentation.
- We build *CAT*, a fully automatic and promptable model that coordinates anatomical prompts derived from 3D cropped volumes with textual prompts enriched by medical domain knowledge, enabling strong flexibility for various segmentation tasks.
- Extensive experiments demonstrate the benefits of coordinating anatomical prompts and textual within one model. *CAT* consistently achieves state-of-the-art performance on multiple segmentation tasks and has generalization capability to diverse tumor types.

2 Related Work

2.1 Textual-prompted Segmentation in Medical Imaging

Prompt engineering has [1, 2] achieved remarkable progress in natural language processing and shown great potential in general visual perception [28–30, 24, 7, 31]. By leveraging pre-trained vision-language foundation models [14], textual-prompted methods demonstrate impressive capabilities in open-vocabulary segmentation [31–36]. These advancements in the natural image field have significantly propelled the field of 2D medical image segmentation [37], where the innovative model architecture is used to recognize a variety of visual contexts through textual prompts. Recently, some efforts tried to train a textual-prompted universal model for segmenting various organs and tumors in 3D volumes [13, 12, 11]. A pre-trained text encoder is adopted to encode the injected prompts and guide the target grounding process. Moreover, the latest attempts [12] focused on extending the short textual phrases with knowledge. However, the reliance on texts struggles with medical image segmentation due to the potential misalignment between textual descriptions and complex visual patterns. To solve the limitations caused by linguistic ambiguity, we integrate visual inputs (i.e., anatomical prompts) for more accurate and comprehensive image perception.

2.2 Visual-prompted Segmentation in Medical Imaging

Beyond textual-prompted methods, the field has seen a notable shift towards incorporating visual prompts to enhance accuracy and context sensitivity [16]. Different from textual prompts, visual prompts introduce more flexibility and context-awareness for models. The innovative Segment Anything [22] introduces a promptable model for generalized image segmentation. Building upon the foundation model, the field has seen a substantial shift towards applying this paradigm to the medical domain. One line adapts SAM to general medical image segmentation with fine-tuning [17, 19–21, 18]. Some works like SAM-Med2D [19] and 3DSAM-adapter [20] utilize adapters [38] to transfer the capabilities of SAM to medical images with a few number of trainable parameters. Other line [39] trains 3D models from scratch straightforwardly. SAM-Med3D [40] and SegVol [39] developed 3D SAM models from scratch by reforming the 2D model and training with a large scale of CT scans. Incorporated with a higher annotated ratio, a 3D point-promptable model CT-SAM3D [41] is introduced with a progressively and spatially aligned prompt encoding technique. Nonetheless, due to the substantial disparities among anomalies in the medical domain, visual prompts could not provide a generic concept for each type. Our work resembles the textual and anatomical prompts to support the multi-organ and tumor segmentation.

3 Method

In this paper, we focus on applying anatomical prompts (i.e., cropped 3D medical volumes) and textual prompts for generic segmentation tasks in the abdomen involving organs and tumors. *CAT* employs a popular query-based encoder-decoder architecture with a sophisticated interaction paradigm between queries and prompts, aiming at predicting N categories in the abdomen, as shown in Figure 2. Our model integrates four main components: i) Vision Backbone, designed to extract image features and construct pixel embedding maps, ii) Prompt Encoders, used to encode anatomical and textual prompts provided by users, respectively, iii) ShareRefiner, utilized to refine segmentation queries and prompt queries, and iv) PromptRefer, generating target queries for prediction.

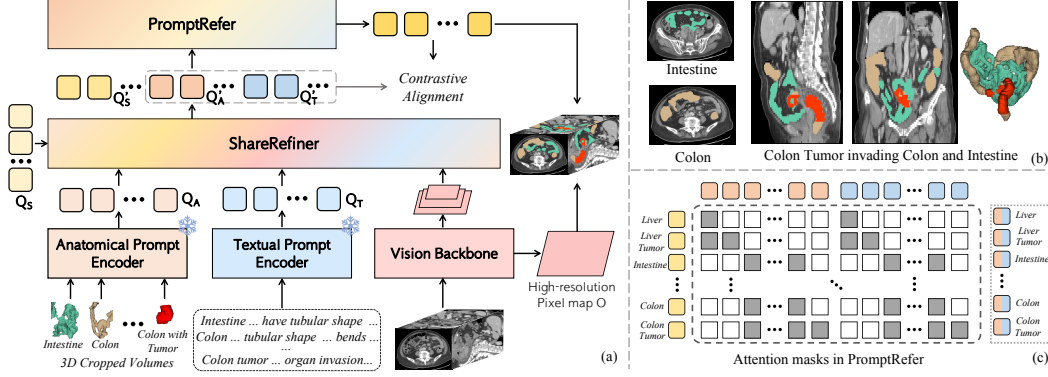


Figure 2: (a) *CAT* follows the query-based segmentation architecture. 3D cropped volumes according to the anatomical structure are utilized as anatomical prompts. Texts enhanced by professional knowledge are adopted as textual prompts. Learnable queries and both prompts are utilized for the final prediction via ShareRefiner and PromptRefer. (b) The case of colon tumor in Stage-IV invading the intestine. (c) Attention masks in PromptRefer for assigning specific prompts to queries.

3.1 Vision Backbone and Prompt Encoders

Backbone. Following other unified models [26, 42] for segmentation tasks, we perform mask classification for all organs and tumors. We adopt a key idea from Mask2Former [42, 12] to construct a pixel embedding map, which is obtained from the backbone encoder features. As shown in Figure 2, the vision backbone comprises a vision encoder **Enc** responsible for extracting multi-scale visual features \mathbf{V} and a vision decoder represented as **Dec**, which gradually upsamples visual features to the high-resolution pixel embedding map O . Given an input 3D volume $I \in \mathbb{R}^{H \times W \times D}$, the process can be formally represented as follows:

$$\mathbf{V} = \text{Enc}(I), O = \text{Dec}(\mathbf{V}), \quad (1)$$

where $\mathbf{V} = \{V^i\}_{i=1}^L$, $V^i \in \mathbb{R}^{H^i \times W^i \times D^i \times C^i}$, and L is the number of layers of the vision encoder. Here, H^i , W^i , D^i and C^i denote the height, width, depth and channel dimension of V^i , respectively. $O \in \mathbb{R}^{H \times W \times D \times C_o}$ is obtained by fusing feature maps from the **Enc**, C_o is the dimension of O .

Prompt Encoders. Prompts have been widely used in segmentation tasks recently. Textual prompts provide comprehensive concepts for the target object but bring some ambiguities, such as the fact that both the intestines and the colon have a “tubular shape”. Conversely, visual prompts are more helpful in disambiguating the user’s intent when textual prompts fail to identify the correct object. However, these visual prompts have limited robustness in handling large variations in medical images [41]. Our method enhances the segmentation process via the coordination of anatomical and textual prompts. Specifically, the anatomical prompt is a referred region from another CT exam, which can be a particular tumor or a cropped volume of the same semantic concept. Given N cropped volumes $P_{Aj} \in \mathbb{R}^{H_A \times W_A \times D_A}$, $j \in \{1, 2, \dots, N\}$, we encode these volumes through a pre-trained encoder **Enc_A** and obtain anatomical prompt embeddings \mathbf{E}_A . To convey the comprehensive notion of targets with detailed information, we utilize long textual descriptions as our textual prompts. Following previous work [12], we incorporate textual prompts with medical domain knowledge. We employ the text encoder **Enc_T** [43] to encode these descriptions and use the [CLS] token output as the textual prompt embedding, denoted as \mathbf{E}_T . The process can be denoted as follows:

$$\mathbf{E}_A = \text{Enc}_A(\mathbf{P}_A), \mathbf{E}_T = \text{Enc}_T(\mathbf{P}_T) \quad (2)$$

$$\mathbf{Q}_A = \text{Linear}(\mathbf{E}_A), \mathbf{Q}_T = \text{Linear}(\mathbf{E}_T), \quad (3)$$

where $\mathbf{Q}_A, \mathbf{Q}_T \in \mathbb{R}^{N \times C}$ are prompt queries and C is the channel dimension.

3.2 ShareRefiner

CAT predicts N masks based on the learnable segmentation queries \mathbf{Q}_S and the pixel embedding map O . Our initial steps involve feeding both segmentation queries \mathbf{Q}_S and prompts queries $\mathbf{Q}_A, \mathbf{Q}_T$

into the proposed ShareRefiner to enable the queries to interact with multi-scale features. In our approach, queries will selectively attend to local image features for self-refinements. Specifically, the ShareRefiner consists of a series of cross-attention blocks where queries perform cross-attention with respect to the target visual feature V^i . To disentangle these queries, we adopt soft and hard assignments for $[\mathbf{Q}_S, \mathbf{Q}_T]$ and \mathbf{Q}_A , respectively. A hard cross-attention layer is applied to extract anatomical prompt features from the multi-scale feature maps, ensuring that each anatomical query gathers discriminative visual regions without overlaps. For the i -th layer of ShareRefiner, the hard assignment similarity matrix of \mathbf{Q}_A^i is computed via Gumbel-Softmax [44, 45] as follows:

$$S^i = \mathbf{Q}_A^i \text{Flatten}(V^i)^T \quad (4)$$

$$S_{\text{gumbel}}^i = \text{Softmax}((S^i + G^i)/\tau), \quad (5)$$

$$S_{\text{onehot}}^i = \text{Onehot}(\text{argmax}_N(S_{\text{gumbel}}^i)). \quad (6)$$

Where $S^i, G^i \in \mathbb{R}^{N \times H^i W^i D^i}$, G^i are i.i.d random samples drawn from the $\text{Gumbel}(0, 1)$ distribution and τ is a learnable coefficient. The one-hot operation of the argmax is performed over S_{gumbel}^i for hard assigning. Since the straightforward hard assignment (i.e., one-hot) is not differentiable, the straight-through trick in [46, 47] is used to compute the assignment similarities S'^i of one-hot value:

$$S'^i = (S_{\text{onehot}}^i)^\top + S_{\text{gumbel}}^i - \text{sg}(S_{\text{gumbel}}^i), \quad (7)$$

where sg denotes the stop gradient operator. Following the feature grouping process, we use a self-attention layer to regulate the relationships among queries and a feed-forward layer for projection. Formally, the aforementioned process is represented as:

$$\mathbf{Q}'_S, \mathbf{Q}'_T = \text{ShareRefiner}([\mathbf{Q}_S, \mathbf{Q}_T], \mathbf{V}, \text{hard} = \text{False}), \quad (8)$$

$$\mathbf{Q}'_A = \text{ShareRefiner}(\mathbf{Q}_A, \mathbf{V}, \text{hard} = \text{True}). \quad (9)$$

3.3 PromptRefer

In practice, when segmenting target objects, more attention needs to be paid to the relevant context. Localizing the typical tumor requires being aware of the anomalous features in the relevant organ, and even identifying organs requires focusing on the anatomical structures involved. For instance, as shown in Figure 2(b), colon tumors of Stage-IV would invade the adjacent organs like intestines. Directly combining prompt queries for mask prediction is suboptimal since there is still an inherent gap between the two types of prompt embeddings even though we have unified them into prompt queries. The typical objective is to classify \mathbf{Q}'_S into respective regions with the guidance of prompts. To this end, we introduce **PromptRefer** implemented by the cross-attention mechanism with carefully crafted attention masks in Figure 2(c). Here, a group of prompt queries $\{Q'_{Ai}, \dots, Q'_{Tj}, \dots\}$ is employed to a specific segmentation query. To ensure the distinction of queries, segmentation queries are required to only interact with queries in the group. This is illustrated in the following equation:

$$\mathbf{O}_S = \text{PromptRefer}([\mathbf{Q}'_S, \mathbf{Q}'_A, \mathbf{Q}'_T], \text{mask}). \quad (10)$$

Here, \mathbf{O}_S represents the decoded segmentation query features for predicting masks.

To further integrate two types of prompts and push segmentation queries closely to the referenced prompt, we employ query-level contrastive learning in our model. Specifically, given the decoded segmentation query features and refined prompt queries, we define two types of losses and calculate the InfoNCE loss [14] as follows:

$$\mathcal{L}_{s2p} = -\frac{1}{N} \sum_{i=1}^N \frac{\exp(\tilde{O}_{Si} \cdot \tilde{Q}'_{\{A/T\}i})}{\sum_{j=0}^N \exp(\tilde{O}_{Si} \cdot \tilde{Q}'_{\{A/T\}j})}, \mathcal{L}_{p2p} = -\frac{1}{N} \sum_{i=1}^N \frac{\exp(\tilde{Q}'_{Ai} \cdot \tilde{Q}'_{Ti})}{\sum_{j=0}^N \exp(\tilde{Q}'_{Ai} \cdot \tilde{Q}'_{Tj})}. \quad (11)$$

Where $\tilde{O}_S, \tilde{Q}'_A, \tilde{Q}'_T$ are derived via linear projection layers. The contrastive alignment can be regarded as a distillation process, whereby each prompt query contributes to the segmentation queries. It also benefits the knowledge exchange between queries from two modalities.

3.4 Training Objective and Strategy

Training Objective. The binary mask proposals $\mathbf{M} \in [0, 1]^{N \times H \times W \times D}$ are calculated through the multiplication operation between the decoded segmentation query features \mathbf{O}_S and the high-resolution pixel embedding map O followed by a Sigmoid. We employ the dice loss for mask

prediction. For classification loss, following [12, 13], we adopt the cross-entropy loss that measures the difference between predicted objects and the categories. Moreover, the contrastive loss is applied to the similarities among queries. The final loss takes the following form:

$$\mathcal{L}_{total} = \mathcal{L}_{dice} + \mathcal{L}_{cls} + \mathcal{L}_{s2p} + \mathcal{L}_{p2p}. \quad (12)$$

Anatomical prompt training strategy. For anatomical prompts, we leverage the bounding box derived from masks in the public dataset and relevant anatomical structures to crop a set of prompt volumes for each category and unify these volumes into the same size. To alleviate the domain shift, we use a pre-trained encoder [48] for feature extraction. During training, we randomly sample an instance from the set of prompt volumes for each category, excluding the identical one.

Textual prompt training strategy. For the textual prompt, we identify the category names in the abdomen. We call GPT-4 [49] to generate descriptions with medical domain knowledge for each category more than 20 times. We recruit one board-certified physician to rewrite the description according to the results. Besides long descriptions for each category, we also construct several short textual templates. We use the long description for the positive category and randomly sample short phrases for those negative categories. More details can be seen in the Appendix A.1.

4 Experiments

Dataset and Settings. *CAT* is trained on the curated dataset from 10 public datasets [50–59], which contain multiple organs and tumors in the abdomen. Following settings in [13], we assemble this dataset with the data pre-processing to reduce the domain gap among various datasets. In the testing phase, two public datasets and one in-house dataset are used for evaluation. The in-house test dataset contains 80 3D CT volumes with colon tumor masks, ranging from Stage-I to Stage-IV. For evaluating the accuracy of organ segmentation, we employ FLARE22 [60] as the external test set. For tumor segmentation, we utilize the combination of MSD dataset [59] and the private dataset. Details of datasets are in Appendix A.2.

Implementation Details and Evaluation Metrics. Our model follows the query-based segmentation architecture [42, 26]. That is, we use Swin UNETR [61] as the backbone and Clinical-Bert [43] as the text-encoder. We follow the experiment settings of previous work [13, 12]. Details are in Appendix A.3. For the evaluation, the Dice Similarity Coefficient (DSC) and 95% Hausdorff Distance (HD95) are utilized to gauge the performance of organ/tumor segmentation.

4.1 Main Results

Organ Segmentation. In this study, we explore the organ segmentation performance of our model on the external testing set of FLARE22. We present the detailed organ-wise segmentation results in Table 1. Compared to models [17, 19] adapting SAM [22] to the medical fields, our approach yields substantially better performance across all 12 organs. For instance, *CAT* significantly surpasses MedSAM [17] by a large margin of 21% DSC points on the adrenal gland segmentation and 15% DSC points on the esophagus segmentation. Such results show the gap in applying 2D SAM-based models for 3D volumes, especially for objects with small sizes or intricate shapes. When compared to 3D SAM models [41, 39, 40], our model performs significantly better than models [39, 40], which take in visual prompts like SAM. For example, we surpass SAM-Med3D [40] and SegVol [39] by 30% points and 20% points in terms of the average score. We can observe that these models also struggle with the problem of handling some difficult organs. In addition, just with one prompt for each category, *CAT* achieves comparable results with CT-SAM3D [41], which utilizes spatially aligned prompts progressively in multi-rounds. Owing to the PromptRefer module, our model demonstrates superior performance in organs where tumors frequently occur. Specifically, *CAT* leads by 2% points in the liver and by 6% points in the pancreas. *CAT* also demonstrates superior performance compared with recent textual-prompted models [13, 12]. Although the gap of organ segmentation is only 2% points, we observed that they do not generalize well on the tumor segmentation task without more intuitive visual prompts, as described in the following part. More details are shown in Table 6.

Tumor Segmentation. We do the evaluation on MSD dataset [59] and an in-house dataset to validate its tumor segmentation capability. Table 2 shows the comparison results of four tumor categories. We do not report HD95 scores for SAM-based methods since this comparison may not be entirely

Table 1: Organ segmentation performance on FLARE22. The results(%) are evaluated by DSC. Scores of SAM-based are adopted from the CT-SAM-Med3D [41]. † denotes obtained via the official pre-trained weights. * means implemented from the official code and trained on the same dataset. Abbreviations: “Liv.”-Liver, “R_Kid.”-Right Kidney, “Spl.”-Spleen, “Pan.”-Pancreas, “Aor.”-Aorta, “IVC”-Inferior Vena Cava, “RAG”-Right Adrenal Gland, “LAG”-Left Adrenal Gland, “Gal.”-Gallbladder, “Eso.”-Esophagus, “Sto.”-Stomach, “Duo.”-Duodenum, “L_Kid.”-Inferior Vena Cava.

Methods	Liv.	R_Kid.	Spl.	Pan.	Aor.	IVC	RAG	LAG	Gal.	Eso.	Sto.	Duo.	L_Kid.	Avg.
SAM [22]	86.0	87.6	84.5	53.4	77.5	44.5	19.4	33.9	52.4	35.2	68.0	44.4	82.6	59.2
MedSAM [17]	93.0	90.0	89.1	73.5	82.5	76.5	36.0	48.7	56.4	64.7	84.0	53.9	89.7	72.2
SAM-Med2D [19]	91.4	83.7	83.9	58.8	60.6	18.6	10.6	27.1	32.9	28.1	72.9	45.4	86.0	53.8
SAM-Med3D [40]	85.4	84.2	84.7	46.9	60.4	44.5	32.6	35.3	56.0	32.6	46.9	27.4	84.9	55.5
SegVol [39]	83.9	71.7	75.9	69.4	83.1	80.3	42.1	49.7	55.6	69.6	81.1	55.6	75.1	68.7
CT-SAM3D [41]	95.6	95.0	96.1	83.6	94.5	91.8	78.4	82.5	88.4	82.9	92.3	73.2	94.8	88.4
Universal† [13]	97.4	95.5	96.4	73.7	84.9	84.4	72.9	73.4	86.0	76.8	88.5	74.5	96.9	84.7
ZePT* [12]	96.7	95.6	96.6	84.3	90.0	84.4	67.2	66.8	79.6	74.2	85.2	59.1	97.2	82.8
CAT	97.7	96.3	97.1	89.2	90.5	88.0	73.6	74.3	83.0	80.1	88.2	73.4	97.3	86.8

Table 2: Segmentation performance (%) of tumors on MSD [59] and In-house dataset. We compare our method with traditional and promptable methods. † denotes obtained via the official pre-trained weights. * means implemented from the official code and trained on the same dataset.

Method	MSD Dataset (Tumor in Abdomen)								In-house Data (Colon Tumor)					
	Liver		Pancreas		Hepatic Vessel		Colon		T1	T2	T3	T4	Avg.	
	DSC↑	HD95↓	DSC↑	HD95↓	DSC↑	HD95↓	DSC↑	HD95↓	DSC↑				DSC↑	HD95↓
nnUNet* [62]	66.42	42.29	43.50	25.80	66.90	47.59	41.41	153.06	19.51	45.06	44.87	45.54	43.00	150.48
Swin UNETR* [48]	68.67	42.54	41.77	22.87	63.32	44.02	39.35	161.26	21.40	33.32	46.11	52.72	45.92	168.25
SAM-Med3D† [40]	44.78	-	40.05	-	44.86	-	39.23	-	34.28	42.65	50.20	42.65	47.11	-
SegVol† [39]	66.20	-	46.36	-	68.57	-	60.63	-	36.93	42.63	60.17	49.83	50.28	-
Universal† [13]	65.68	63.31	45.72	16.58	66.31	51.47	42.26	115.40	7.11	43.28	46.52	53.08	47.14	140.28
ZePT* [12]	68.58	43.23	44.39	19.47	68.12	33.94	40.38	113.07	23.87	34.64	50.81	51.09	46.28	155.83
CAT	72.73	34.64	49.67	15.56	70.11	33.44	48.31	108.26	30.62	45.61	55.85	57.37	53.35	80.96

equitable. Our **CAT** outperforms baselines [62, 48] significantly across all tumor subtypes, achieving at least a 4% improvement in DSC. For the comparison of SAM-based methods [40, 39], it is worth noting that only one point derived from the ground truths is utilized as the prompt during the inference time since tumors of small sizes are difficult to identify but can be easily segmented with the provided prompts. Without using information from labels, **CAT** still achieves better performance except for the colon tumor segmentation, as evidenced by a 5% improvement in the DSC of the pancreas tumor. These results validate the proposed PromptRefer module (i.e., attending to specific organs when segmenting tumors). Moreover, we compare **CAT** with textual-prompted methods. **CAT** surpasses the previously across four tasks by 4% in the average DSC. As our model is an extension of textual-prompted methods, these results demonstrate that incorporating the anatomical prompts can produce higher-quality masks for tumors. More details are shown in Table 7.

We further conduct the evaluation on an in-house colon tumor dataset, with tumors ranging from Stage-I (T1) to Stage-IV (T4) according to the Cancer Staging System [23]. As shown in Table 2, **CAT** showcases strong capabilities in dealing with tumors of diverse sizes and shapes. To provide deeper insight, we present the average score of each subtype. It is noted that the higher the number after the “T”, the larger the tumor or the more extensively it has grown into nearby tissues. We can observe that SAM-derived methods perform well in segmenting relatively small T1 tumors with point prompts. However, SegVol [39], which achieves the best results in MSD colon tumor segmentation, struggles to handle tumors that invade nearby organs or tissues. It is evident from the performance gap between T3 and T4 tumors. In these cases, tumors in each instance can present with varying densities and show distinct shapes at different locations. Only using visual prompts without comprehensive descriptions to cover all abnormal parts proves challenging. Such scenarios are vital in the medical field, highlighting the need for further research in applying visual prompts for tumor segmentation. In this paper, we coordinate anatomical and textual prompts along with the predefined attention mask to alleviate this problem. **CAT** outperforms other models by at least absolute 7% DSC in T4 and 3% DSC on average, demonstrating much better generalizability and robustness. This result suggests that leveraging anatomical prompts together with medical domain knowledge is an alternative way to address intricate scenarios in the medical domain.

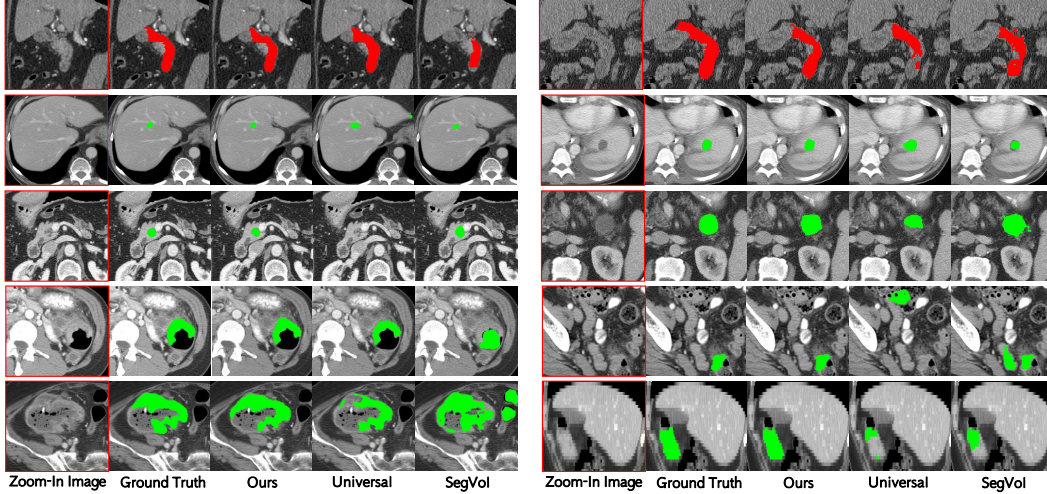


Figure 3: Qualitative visualizations of the proposed model and other prompting methods on **organ/tumor** segmentation. The segmentation results presented from rows one to five correspond, in order, to the duodenum, liver tumors, pancreas tumors, colon tumors, and colon tumors in Stage-IV.

Qualitative Comparison. To give more intuitive comparisons, we present the qualitative results in Figure 3. In the first row, we observe that current methods may struggle with segmenting tubular-shaped organs, particularly SAM-derived methods like SegVol [39], since visual prompts can not convey the general concept of such tubular-shaped objects. The results in the second and third rows reveal that textual-prompted models are prone to misclassification and overlook key details due to the lack of intuitive context, underscoring the importance of visual prompts. However, these only relying on visual prompts struggle with tumors of intricate shapes without the support of medical domain knowledge, as shown in the fourth row, where SegVol exhibits a high number of false positives on normal CT scans. When tumors invade other tissues, existing models often fail due to segmentation target incompleteness and misclassification of normal regions as tumors. In contrast, *CAT* can precisely identify most abnormal regions and consistently generate results that are more consistent with the ground truth compared to all other models.

4.2 Ablation Studies

To fully investigate the contribution of our introduced components, we conducted ablation studies to compare each part in both organ and tumor segmentation tasks. We selected a subset of organ and tumor categories that are particularly challenging for models, facilitating a more intuitive comparison.

Ablation of Two Prompts. We start from a basic query-based segmentation architecture without any extra prompts, and then we ablate the effectiveness of using different prompts for different tasks. As demonstrated in Table 3 (the first four rows), eliminating the prompt schema leads to a substantial performance drop on both organ and tumor segmentation ($64.08 \rightarrow 54.39$ in Duodenum and $72.49 \rightarrow 66.37$ in Liver tumor). The observed declines in the third row indicate that textual features, which are rich in semantics but lack appearance features, may not generalize well to objects with intricate structures or small sizes. It is evidenced by a performance reduction of 6% in Esophagus segmentation and 4% in Hepatic Vessel tumor segmentation. Moreover, we can observe from the second row that the tumor segmentation capability is inadequate when relying solely on anatomical prompts. This issue stems from the diversity and variance of tumors. For instance, every example the model encounters is drastically different as it tries to identify the location and nature of pancreas tumor. Although tumors can be regarded as anomalies, the lack of consistent context poses a challenge for the model in establishing a general concept solely with the cropped volumes. The coordination of anatomical and textual prompts improves the performance of the promptable model. This confirms the efficacy of our joint prompts schema, which is designed to help the model form more stable and generalizable masks in the medical field.

Table 3: Ablation studies of two prompts and model designs on organ and tumor segmentation dataset.

Variant				Organ (%)					Tumor (%)				
AP	TP	Hard	Mask	Pan.	RAG	LAG	Eso.	Duo.	Liver	Pancreas	HepVes.	Colon	T4
✓				78.18	69.63	69.08	76.99	54.39	66.37	42.05	62.20	39.85	51.17
	✓			83.55	72.80	71.65	79.31	60.45	64.82	45.08	68.72	43.84	53.91
		✓		80.62	71.02	70.34	72.81	57.31	69.13	44.31	65.18	40.16	52.32
✓	✓			83.50	72.71	69.96	78.99	64.08	72.49	44.55	69.40	44.50	55.84
			✓	86.74	72.41	69.00	77.68	59.99	69.12	43.23	67.75	41.32	54.33
✓	✓	✓		87.36	74.46	74.02	75.39	70.80	72.64	48.49	69.02	47.29	53.67
✓	✓		✓	88.49	73.24	74.51	80.76	70.26	72.18	46.46	69.97	46.65	58.49
✓	✓	✓	✓	88.28	74.42	72.50	79.30	71.26	70.95	45.52	69.51	46.07	56.41
✓	✓	✓	✓	89.24	73.69	74.63	80.10	73.46	72.73	49.67	70.11	48.31	57.37



Figure 4: T-SNE visualization of the distribution of Features. Left: Two types of prompt embedding before and after refinement. Right: Segmentation query features with and without constrastive alignment. (1-9: right kidney, left kidney, liver, pancreas, colon, kidney tumor, liver tumor, pancreas tumor, colon tumor).

Effectiveness of Module Designs. As presented in the last five rows in Table 3, we evaluate the impacts of the module designs in our ShareRefiner and PromptRefer. The comparison of results between the seventh and last rows demonstrates that employing the hard assignment for refining the anatomical queries can boost performances, especially for tumor segmentation. However, applying the paradigm to the other two queries (i.e., the ‘Hard’ column is marked as ✓) will decrease the performance of segmentation. This decline can be attributed to the entanglement of the three query types. Such a phenomenon further reinforces that anatomical and textual prompts contribute from different perspectives. Using a one-hot hard assignment ensures that each query feature remains exclusive to the others, allowing queries to focus on distinct visual regions without overlap. We hypothesize that anatomical queries could attend to features and distinguish between different categories based on inherent appearance characteristics. Additionally, we remove the mask mechanism in the PromptRefer and utilize a vanilla cross-attention layer to update \mathbf{Q}'_S . As illustrated in Table 3, this variant leads to reduced performance in tumors that invade other organs (e.g., Stage-IV). The result verifies that guiding queries to focus on relevant objects is an effective strategy for achieving more robust segmentation in medical scenarios.

Visualizations. We select nine categories (five organs and four tumors) and use t-SNE [63] to visualize the distribution of prompt features (\mathbf{E}_A and \mathbf{E}_T) and updated prompts queries (\mathbf{Q}'_A and \mathbf{Q}'_T) in Figure 4. Our findings indicate that the initial prompt features are not well-separated in the feature space. For instance, the anatomical features of the right kidney and left kidney (categories 1 and 2) are entangled. Therefore, different refined paradigms need to be applied to update both queries simultaneously. With our ShareRefiner, prompt features are separated in the feature space. Moreover, we can observe that the distribution of refined anatomical prompt queries is more structured than textual prompts, which further verifies that the anatomical prompt is more intuitive. Contrastive alignment is utilized to further push segmentation queries to be close to the referenced prompt for segmenting the corresponding category. To validate the effectiveness, we trained without utilizing contrastive alignment. We also use t-SNE to visualize the distribution of decoded segmentation query features \mathbf{O}_S in the right part of Figure 4. We can observe that segmentation queries are more separated in the feature space with contrastive alignment. Additionally, we visualize the heatmaps derived from experiments in the second and third rows of Table 3. As shown in Figure 5, solely using textual prompts fails to cover all regions, while only relying on anatomical prompts results in a high

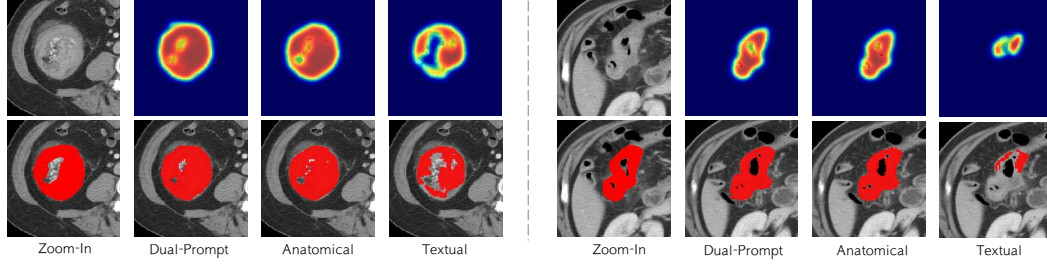


Figure 5: Heatmaps of two samples for analyzing the effectiveness of two prompts.

false positive rate. These visual examples underscore the importance of combining both types of prompts to guide medical image segmentation effectively.

5 Conclusion and Discussion

Conclusion. We present *CAT*, a promising attempt towards comprehensive medical segmentation via coordinating anatomical-textual prompts. Apart from performing generic organ segmentation, *CAT* can identify varying tumors without human interaction. To effectively integrate two prompt modalities into a single model, we design ShareRefiner to refine latent prompt queries with different strategies and introduce PromptRefer with specific attention masks to assign prompts to segmentation queries for mask prediction. Extensive experiments indicate that the coordination of these two prompt modalities yields competitive performance on organ and tumor segmentation benchmarks. Further studies revealed the robust generalization capabilities to segment tumors in different cancer stages. We hope our early exploration of the complementary advantages between anatomical and textual prompts could bring new insights into the field of the community.

Limitation and Impact. We hope our model can support professionals in the arduous clinical diagnosis process. Despite the integration of anatomical and textual prompts showing competitive performance in the segmentation tasks, the lack of general anatomical prompts encoders raises challenges, as indicated by the messy distribution of initial anatomical embeddings. Therefore, further research into improving the CT foundation models is essential. Moreover, there may also be mistakes in the segmentation results, especially when the test sample contains rare types of lesions or undergoes radical resection surgeries that cause large variations in the anatomical structures. Therefore, before integrating these AI-based algorithms into clinical practice, legislation needs to be developed and implemented to ensure that there are clear guidelines and standards for their use.

Acknowledgments and Disclosure of Funding

This work was supported by the National Natural Science Foundation of China (No. 62301311) and the Shanghai Municipal Commission of Economy and Informatization (No. 204694).

References

- [1] Tom Brown, Benjamin Mann, Nick Ryder, Melanie Subbiah, Jared D Kaplan, Prafulla Dhariwal, Arvind Neelakantan, Pranav Shyam, Girish Sastry, Amanda Askell, et al. Language models are few-shot learners. *Advances in neural information processing systems*, 33:1877–1901, 2020.
- [2] Jason Wei, Xuezhi Wang, Dale Schuurmans, Maarten Bosma, Fei Xia, Ed Chi, Quoc V Le, Denny Zhou, et al. Chain-of-thought prompting elicits reasoning in large language models. *Advances in neural information processing systems*, 35:24824–24837, 2022.
- [3] Josh Achiam, Steven Adler, Sandhini Agarwal, Lama Ahmad, Ilge Akkaya, Florencia Leoni Aleman, Diogo Almeida, Janko Altenschmidt, Sam Altman, Shyamal Anadkat, et al. Gpt-4 technical report. *arXiv preprint arXiv:2303.08774*, 2023.

- [4] Hugo Touvron, Louis Martin, Kevin Stone, Peter Albert, Amjad Almahairi, Yasmine Babaei, Nikolay Bashlykov, Soumya Batra, Prajjwal Bhargava, Shruti Bhosale, et al. Llama 2: Open foundation and fine-tuned chat models. *arXiv preprint arXiv:2307.09288*, 2023.
- [5] Gemini Team, Rohan Anil, Sebastian Borgeaud, Yonghui Wu, Jean-Baptiste Alayrac, Jiahui Yu, Radu Soricut, Johan Schalkwyk, Andrew M Dai, Anja Hauth, et al. Gemini: a family of highly capable multimodal models. *arXiv preprint arXiv:2312.11805*, 2023.
- [6] Chunyuan Li, Zhe Gan, Zhengyuan Yang, Jianwei Yang, Linjie Li, Lijuan Wang, and Jianfeng Gao. Multi-modal foundation models: From specialists to general-purpose assistants. *arXiv preprint arXiv:2309.10020*, 1(2):2, 2023.
- [7] Feng Li, Qing Jiang, Hao Zhang, Tianhe Ren, Shilong Liu, Xueyan Zou, Huaizhe Xu, Hongyang Li, Chunyuan Li, Jianwei Yang, et al. Visual in-context prompting. *arXiv preprint arXiv:2311.13601*, 2023.
- [8] Ehab A AlBadawy, Ashirbani Saha, and Maciej A Mazurowski. Deep learning for segmentation of brain tumors: Impact of cross-institutional training and testing. *Medical physics*, 45(3):1150–1158, 2018.
- [9] Mohammad Hesam Hesamian, Wenjing Jia, Xiangjian He, and Paul Kennedy. Deep learning techniques for medical image segmentation: achievements and challenges. *Journal of digital imaging*, 32:582–596, 2019.
- [10] Shaoting Zhang and Dimitris Metaxas. On the challenges and perspectives of foundation models for medical image analysis. *Medical Image Analysis*, page 102996, 2023.
- [11] Ziheng Zhao, Yao Zhang, Chaoyi Wu, Xiaoman Zhang, Ya Zhang, Yanfeng Wang, and Weidi Xie. One model to rule them all: Towards universal segmentation for medical images with text prompts. *arXiv preprint arXiv:2312.17183*, 2023.
- [12] Yankai Jiang, Zhongzhen Huang, Rongzhao Zhang, Xiaofan Zhang, and Shaoting Zhang. Zept: Zero-shot pan-tumor segmentation via query-disentangling and self-prompting. *arXiv preprint arXiv:2312.04964*, 2023.
- [13] Jie Liu, Yixiao Zhang, Jie-Neng Chen, Junfei Xiao, Yongyi Lu, Bennett A Landman, Yixuan Yuan, Alan Yuille, Yucheng Tang, and Zongwei Zhou. Clip-driven universal model for organ segmentation and tumor detection. *arXiv preprint arXiv:2301.00785*, 2023.
- [14] Alec Radford, Jong Wook Kim, Chris Hallacy, Aditya Ramesh, Gabriel Goh, Sandhini Agarwal, Girish Sastry, Amanda Askell, Pamela Mishkin, Jack Clark, et al. Learning transferable visual models from natural language supervision. In *International conference on machine learning*, pages 8748–8763. PMLR, 2021.
- [15] Jacob Devlin, Ming-Wei Chang, Kenton Lee, and Kristina Toutanova. Bert: Pre-training of deep bidirectional transformers for language understanding. *arXiv preprint arXiv:1810.04805*, 2018.
- [16] Victor Ion Butoi, Jose Javier Gonzalez Ortiz, Tianyu Ma, Mert R Sabuncu, John Guttag, and Adrian V Dalca. Universeg: Universal medical image segmentation. In *Proceedings of the IEEE/CVF International Conference on Computer Vision*, pages 21438–21451, 2023.
- [17] Jun Ma, Yuting He, Feifei Li, Lin Han, Chenyu You, and Bo Wang. Segment anything in medical images. *Nature Communications*, 15(1):654, 2024.
- [18] Cheng Chen, Juzheng Miao, Dufan Wu, Zhiling Yan, Sekeun Kim, Jiang Hu, Aoxiao Zhong, Zhengliang Liu, Lichao Sun, Xiang Li, et al. Ma-sam: Modality-agnostic sam adaptation for 3d medical image segmentation. *arXiv preprint arXiv:2309.08842*, 2023.
- [19] Junlong Cheng, Jin Ye, Zhongying Deng, Jianpin Chen, Tianbin Li, Haoyu Wang, Yanzhou Su, Ziyan Huang, Jilong Chen, Lei Jiang, et al. Sam-med2d. *arXiv preprint arXiv:2308.16184*, 2023.
- [20] Shizhan Gong, Yuan Zhong, Wenao Ma, Jinpeng Li, Zhao Wang, Jingyang Zhang, Pheng-Ann Heng, and Qi Dou. 3dsam-adapter: Holistic adaptation of sam from 2d to 3d for promptable medical image segmentation. *arXiv preprint arXiv:2306.13465*, 2023.
- [21] Kaidong Zhang and Dong Liu. Customized segment anything model for medical image segmentation. *arXiv preprint arXiv:2304.13785*, 2023.
- [22] Alexander Kirillov, Eric Mintun, Nikhila Ravi, Hanzi Mao, Chloe Rolland, Laura Gustafson, Tete Xiao, Spencer Whitehead, Alexander C Berg, Wan-Yen Lo, et al. Segment anything. In *Proceedings of the IEEE/CVF International Conference on Computer Vision*, pages 4015–4026, 2023.

- [23] National Cancer Institute. Cancer staging, 2022. Accessed: 2024-05-21.
- [24] Xueyan Zou, Jianwei Yang, Hao Zhang, Feng Li, Linjie Li, Jianfeng Wang, Lijuan Wang, Jianfeng Gao, and Yong Jae Lee. Segment everything everywhere all at once. *Advances in Neural Information Processing Systems*, 36, 2024.
- [25] Feng Li, Hao Zhang, Huaizhe Xu, Shilong Liu, Lei Zhang, Lionel M Ni, and Heung-Yeung Shum. Mask dino: Towards a unified transformer-based framework for object detection and segmentation. In *Proceedings of the IEEE/CVF Conference on Computer Vision and Pattern Recognition*, pages 3041–3050, 2023.
- [26] Bowen Cheng, Ishan Misra, Alexander G Schwing, Alexander Kirillov, and Rohit Girdhar. Masked-attention mask transformer for universal image segmentation. In *Proceedings of the IEEE/CVF conference on computer vision and pattern recognition*, pages 1290–1299, 2022.
- [27] Huiyu Wang, Yukun Zhu, Hartwig Adam, Alan Yuille, and Liang-Chieh Chen. Max-deeplab: End-to-end panoptic segmentation with mask transformers. In *Proceedings of the IEEE/CVF conference on computer vision and pattern recognition*, pages 5463–5474, 2021.
- [28] Xiuye Gu, Tsung-Yi Lin, Weicheng Kuo, and Yin Cui. Open-vocabulary object detection via vision and language knowledge distillation. *arXiv preprint arXiv:2104.13921*, 2021.
- [29] Shilong Liu, Zhaoyang Zeng, Tianhe Ren, Feng Li, Hao Zhang, Jie Yang, Chunyuan Li, Jianwei Yang, Hang Su, Jun Zhu, et al. Grounding dino: Marrying dino with grounded pre-training for open-set object detection. *arXiv preprint arXiv:2303.05499*, 2023.
- [30] Jiarui Xu, Sifei Liu, Arash Vahdat, Wonmin Byeon, Xiaolong Wang, and Shalini De Mello. Open-vocabulary panoptic segmentation with text-to-image diffusion models. In *Proceedings of the IEEE/CVF Conference on Computer Vision and Pattern Recognition*, pages 2955–2966, 2023.
- [31] Hao Zhang, Feng Li, Xueyan Zou, Shilong Liu, Chunyuan Li, Jianwei Yang, and Lei Zhang. A simple framework for open-vocabulary segmentation and detection. In *Proceedings of the IEEE/CVF International Conference on Computer Vision*, pages 1020–1031, 2023.
- [32] Jian Ding, Nan Xue, Gui-Song Xia, and Dengxin Dai. Decoupling zero-shot semantic segmentation. In *Proceedings of the IEEE/CVF Conference on Computer Vision and Pattern Recognition*, pages 11583–11592, 2022.
- [33] Feng Liang, Bichen Wu, Xiaoliang Dai, Kunpeng Li, Yinan Zhao, Hang Zhang, Peizhao Zhang, Peter Vajda, and Diana Marculescu. Open-vocabulary semantic segmentation with mask-adapted clip. In *Proceedings of the IEEE/CVF Conference on Computer Vision and Pattern Recognition*, pages 7061–7070, 2023.
- [34] Golnaz Ghiasi, Xiuye Gu, Yin Cui, and Tsung-Yi Lin. Scaling open-vocabulary image segmentation with image-level labels. In *European Conference on Computer Vision*, pages 540–557. Springer, 2022.
- [35] Mengde Xu, Zheng Zhang, Fangyun Wei, Yutong Lin, Yue Cao, Han Hu, and Xiang Bai. A simple baseline for open-vocabulary semantic segmentation with pre-trained vision-language model. In *European Conference on Computer Vision*, pages 736–753. Springer, 2022.
- [36] Jie Qin, Jie Wu, Pengxiang Yan, Ming Li, Ren Yuxi, Xuefeng Xiao, Yitong Wang, Rui Wang, Shilei Wen, Xin Pan, et al. Freeseg: Unified, universal and open-vocabulary image segmentation. In *Proceedings of the IEEE/CVF Conference on Computer Vision and Pattern Recognition*, pages 19446–19455, 2023.
- [37] Shiyi Du, Xiaosong Wang, Yongyi Lu, Yuyin Zhou, Shaoting Zhang, Alan Yuille, Kang Li, and Zongwei Zhou. Boosting dermatoscopic lesion segmentation via diffusion models with visual and textual prompts. *arXiv preprint arXiv:2310.02906*, 2023.
- [38] Edward J Hu, Yelong Shen, Phillip Wallis, Zeyuan Allen-Zhu, Yuanzhi Li, Shean Wang, Lu Wang, and Weizhu Chen. Lora: Low-rank adaptation of large language models. *arXiv preprint arXiv:2106.09685*, 2021.
- [39] Yuxin Du, Fan Bai, Tiejun Huang, and Bo Zhao. Segvol: Universal and interactive volumetric medical image segmentation. *arXiv preprint arXiv:2311.13385*, 2023.
- [40] Haoyu Wang, Sizheng Guo, Jin Ye, Zhongying Deng, Junlong Cheng, Tianbin Li, Jianpin Chen, Yanzhou Su, Ziyang Huang, Yiqing Shen, et al. Sam-med3d. *arXiv preprint arXiv:2310.15161*, 2023.

- [41] Heng Guo, Jianfeng Zhang, Jiaxing Huang, Tony CW Mok, Dazhou Guo, Ke Yan, Le Lu, Dakai Jin, and Minfeng Xu. Towards a comprehensive, efficient and promptable anatomic structure segmentation model using 3d whole-body ct scans. *arXiv preprint arXiv:2403.15063*, 2024.
- [42] Bowen Cheng, Alex Schwing, and Alexander Kirillov. Per-pixel classification is not all you need for semantic segmentation. *Advances in neural information processing systems*, 34:17864–17875, 2021.
- [43] Emily Alsentzer, John R Murphy, Willie Boag, Wei-Hung Weng, Di Jin, Tristan Naumann, and Matthew McDermott. Publicly available clinical bert embeddings. *arXiv preprint arXiv:1904.03323*, 2019.
- [44] Eric Jang, Shixiang Gu, and Ben Poole. Categorical reparameterization with gumbel-softmax. In *ICLR*, 2017.
- [45] Chris J Maddison, Andriy Mnih, and Yee Whye Teh. The concrete distribution: A continuous relaxation of discrete random variables. In *ICLR*, 2017.
- [46] Aaron Van Den Oord, Oriol Vinyals, et al. Neural discrete representation learning. *Advances in neural information processing systems*, 30, 2017.
- [47] Jiarui Xu, Shalini De Mello, Sifei Liu, Wonmin Byeon, Thomas Breuel, Jan Kautz, and Xiaolong Wang. Groupvit: Semantic segmentation emerges from text supervision. In *Proceedings of the IEEE/CVF Conference on Computer Vision and Pattern Recognition*, pages 18134–18144, 2022.
- [48] Yucheng Tang, Dong Yang, Wenqi Li, Holger R Roth, Bennett Landman, Daguang Xu, Vishwesh Nath, and Ali Hatamizadeh. Self-supervised pre-training of swin transformers for 3d medical image analysis. In *CVPR*, pages 20730–20740, 2022.
- [49] OpenAI. Gpt-4 technical report, 2023.
- [50] Bennett Landman, Zhoubing Xu, J Igelsias, Martin Styner, T Langerak, and Arno Klein. Miccai multi-atlas labeling beyond the cranial vault—workshop and challenge. In *Proc. MICCAI Multi-Atlas Labeling Beyond Cranial Vault—Workshop Challenge*, volume 5, page 12, 2015.
- [51] Yuanfeng Ji, Haotian Bai, Chongjian Ge, Jie Yang, Ye Zhu, Ruimao Zhang, Zhen Li, Lingyan Zhanng, Wanling Ma, Xiang Wan, et al. Amos: A large-scale abdominal multi-organ benchmark for versatile medical image segmentation. *Advances in Neural Information Processing Systems*, 35:36722–36732, 2022.
- [52] A Emre Kavur, N Sinem Gezer, Mustafa Barış, Sinem Aslan, Pierre-Henri Conze, Vladimir Groza, Duc Duy Pham, Soumick Chatterjee, Philipp Ernst, Savaş Özkan, et al. Chaos challenge-combined (ct-mr) healthy abdominal organ segmentation. *Medical Image Analysis*, 69:101950, 2021.
- [53] Blaine Rister, Darvin Yi, Kaushik Shivakumar, Tomomi Nobashi, and Daniel L Rubin. Ct-org, a new dataset for multiple organ segmentation in computed tomography. *Scientific Data*, 7(1):381, 2020.
- [54] Jun Ma, Yao Zhang, Song Gu, Cheng Zhu, Cheng Ge, Yichi Zhang, Xingle An, Congcong Wang, Qiyuan Wang, Xin Liu, et al. Abdomenct-1k: Is abdominal organ segmentation a solved problem. *IEEE TPAMI*, 2021.
- [55] Holger R Roth, Le Lu, Amal Farag, Hoo-Chang Shin, Jiamin Liu, Evrim B Turkbey, and Ronald M Summers. Deeporgan: Multi-level deep convolutional networks for automated pancreas segmentation. In *Medical Image Computing and Computer-Assisted Intervention—MICCAI 2015: 18th International Conference, Munich, Germany, October 5-9, 2015, Proceedings, Part I 18*, pages 556–564. Springer, 2015.
- [56] Xiangde Luo, Wenjun Liao, Jianghong Xiao, Jieneng Chen, Tao Song, Xiaofan Zhang, Kang Li, Dimitris N Metaxas, Guotai Wang, and Shaoting Zhang. Word: A large scale dataset, benchmark and clinical applicable study for abdominal organ segmentation from ct image. *Medical Image Analysis*, 82:102642, 2022.
- [57] Patrick Bilic, Patrick Christ, Hongwei Bran Li, Eugene Vorontsov, Avi Ben-Cohen, Georgios Kaissis, Adi Szeskin, Colin Jacobs, Gabriel Efrain Humpire Mamani, Gabriel Chartrand, et al. The liver tumor segmentation benchmark (lits). *Medical Image Analysis*, 84:102680, 2023.
- [58] Nicholas Heller, Sean McSweeney, Matthew Thomas Peterson, Sarah Peterson, Jack Rickman, Bethany Stai, Resha Tejapaul, Makinna Oestreich, Paul Blake, Joel Rosenberg, et al. An international challenge to use artificial intelligence to define the state-of-the-art in kidney and kidney tumor segmentation in ct imaging., 2020.
- [59] Michela Antonelli, Annika Reinke, Spyridon Bakas, Keyvan Farahani, Annette Kopp-Schneider, Bennett A Landman, Geert Litjens, Bjoern Menze, Olaf Ronneberger, Ronald M Summers, et al. The medical segmentation decathlon. *Nature communications*, 13(1):4128, 2022.

- [60] Jun Ma, Yao Zhang, Song Gu, Cheng Ge, Shihao Ma, Adamo Young, Cheng Zhu, Kangkang Meng, Xin Yang, Ziyang Huang, Fan Zhang, Wentao Liu, YuanKe Pan, Shoujin Huang, Jiacheng Wang, Mingze Sun, Weixin Xu, Dengqiang Jia, Jae Won Choi, Natália Alves, Bram de Wilde, Gregor Koehler, Yajun Wu, Manuel Wiesenfarth, Qiongjie Zhu, Guoqiang Dong, Jian He, the FLARE Challenge Consortium, and Bo Wang. Unleashing the strengths of unlabeled data in pan-cancer abdominal organ quantification: the flare22 challenge. *arXiv preprint arXiv:2308.05862*, 2023.
- [61] Ali Hatamizadeh, Vishwesh Nath, Yucheng Tang, Dong Yang, Holger R Roth, and Daguang Xu. Swin unetr: Swin transformers for semantic segmentation of brain tumors in mri images. In *International MICCAI Brainlesion Workshop*, pages 272–284. Springer, 2021.
- [62] Fabian Isensee, Paul F Jaeger, Simon AA Kohl, Jens Petersen, and Klaus H Maier-Hein. nnu-net: a self-configuring method for deep learning-based biomedical image segmentation. *Nature methods*, 18(2):203–211, 2021.
- [63] Laurens Van der Maaten and Geoffrey Hinton. Visualizing data using t-sne. *Journal of machine learning research*, 9(11), 2008.
- [64] Ilya Loshchilov and Frank Hutter. Decoupled weight decay regularization. *arXiv preprint arXiv:1711.05101*, 2017.

A Appendix / supplemental material

A.1 Textual Prompts Construction

The instruction for GPT-4	Short phrase templates
Please describe the provided organs and tumors. Descriptions should include the location, its anatomical structure, common pathological findings, and common tumors (for organs). Answers must be based on observations from CT imaging.	A computerized tomography of a [CLS]. A photo of a [CLS]. There is [CLS] in this computerized tomography. [CLS]

Table 4: The strategy of constructing textual prompts.

We call GPT-4 to generate long descriptions for each category and use templates to construct some short textual prompts, as shown in Table A.1. We use the long description for the positive category and randomly sample short phrases for those negative categories. Positive categories indicate labeled categories in the case.

A.2 Dataset Details

The overall categories used in our paper consist of 23 organs and 6 anomalies. The test set of MSD is the same as the official code of [13]. Details of utilized datasets are shown as follows:

- (1) The BTCV dataset [50] consists of 30 abdominal CT scans from 13 annotated organs, conducted under the supervision of radiologists at Vanderbilt University Medical Center.
- (2) The CT-ORG dataset [53] encompasses 140 CT images, featuring six organ classes. These images primarily display liver lesions, including both benign and malignant types.
- (3) The AbdomenCT-1K dataset [54] comprises 1,112 CT scans pooled from five datasets, annotated for the liver, kidney, spleen, and pancreas.
- (4) CHAOS [52] offers 40 CT scans of healthy abdominal organs for multi-organ segmentation, specifically excluding any pathological abnormalities such as tumors or metastasis.
- (5) AMOS22 [51], a multi-modality abdominal multi-organ segmentation challenge of 2022, includes 500 CT scans with voxel-level annotations of 15 abdominal organs.
- (6) The WORD dataset [56] collects 150 CT scans from patients prior to radiation therapy at a single center, with each volume consisting of 159 to 330 slices and comprehensively annotated for 16 anatomical organs.
- (7) Pancreas-CT [55] contains 82 contrast-enhanced abdominal CT volumes focused solely on the pancreas, annotated by an experienced radiologist and excluding any pancreatic tumors.
- (8) The LiTS dataset [57] comprises 201 contrast-enhanced abdominal CT scans (131 for training and 70 for testing), acquired across six clinical sites using various scanners and protocols, with a resolution range from 0.55 to 1.0 mm and slice spacing from 0.45 to 6.0 mm.
- (9) KiTS [58] includes 300 CT scans (210 for training and 90 for testing) with annotations provided by the University of Minnesota Medical Center, each featuring one or more kidney tumors.
- (10) The Medical Segmentation Decathlon (MSD) [59] comprises 947 CT scans targeting liver, lung, pancreas, colon, hepatic vessels, and spleen, encompassing a total of four organs and five tumors.
- (11) Our in-house dataset contains 80 CT scans of patients diagnosed with colon cancer, annotated by an experienced gastroenterologist and verified by a senior radiologist. All scans maintain a consistent in-plane dimension of 512×512 pixels, while the z-axis dimension ranges from 36 to 146, with a median of 91. **Note that there are some cases where the cancer stage can not be identified.**

A.3 Implementation Details

AdamW optimizer [64] is utilized as the optimizer. The default initial learning rate is 1×10^{-4} , and we decay it following the learning rate scheduling strategy of [61]. Each volume is cropped into patches with a size of $96 \times 96 \times 96$. Random shift, zoom and scale, and scaling are applied on-the-fly to improve the generalization. Our framework is implemented using PyTorch and all experiments are

Datasets	#Scans	Annotated categories
BTCV [50]	30	Spl, RKid, LKid, Gall, Eso, Liv, Sto, Aor, IVC, R&SVeins, Pan, RAG, LAG
CT-ORG [53]	140	Lung, Liver, Kidneys and Bladder
AbdomenCT-1K [54]	1000	Spleen, Kidney, Liver, Pancreas
CHAOS [52]	40	Liver, Left Kidney, Right Kidney, Spleen
AMOS22 [51]	500	Spl, RKid, LKid, Gall, Eso, Liv, Sto, Aor, IVC, Pan, RAG, LAG, Duo, Bla, Pro/UTE
WORD [56]	150	Spl, RKid, LKid, Gall, Eso, Liv, Sto, Pan, RAG, Duo, Col, Int, Rec, Bla, LFH, RFH
Pancreas-CT [55]	82	Pancreas
LiTS [57]	201	Liver, <i>Liver Tumor</i>
KiTS [58]	300	Kidney, <i>Kidney Tumor</i>
MSD CT Tasks [59]	947	Spl, Liver, <i>Liver Tumor</i> , <i>Lung Tumor</i> , <i>Colon Tumor</i> , Pancreas and <i>Pancreas Tumor</i> , Hepatic Vessel and <i>Hepatic Vessel Tumor</i>
In-house dataset	80	<i>Colon Tumor</i> with four subtypes

Table 5: The information for all datasets.

conducted on 8 NVIDIA A100 GPUs. For the evaluation, the Dice Similarity Coefficient (DSC) and 95% Hausdorff Distance (HD95) are utilized to gauge the performance of organ/tumor segmentation.

A.4 Results Details

Table 6: Organ segmentation performance on FLARE22. The results(%) are evaluated by DSC. Scores of SAM-based are adopted from the CT-SAM-Med3D [41]. † denotes obtained via the official pre-trained weights. * means implemented from the official code and trained on the same dataset. Abbreviations: “Liv.”-Liver, “R_Kid.”-Right Kidney, “Spl.”-Spleen, “Pan.”-Pancreas, “Aor.”-Aorta, “IVC”-Inferior Vena Cava, “RAG”-Right Adrenal Gland, “LAG”-Left Adrenal Gland, “Gal.”-Gallbladder, “Eso.”-Esophagus, “Sto.”-Stomach, “Duo.”-Duodenum, “L_Kid.”-Inferior Vena Cava.

Methods	Liv.	R_Kid.	Spl.	Pan.	Aor.	IVC	RAG	LAG	Gal.	Eso.	Sto.	Duo.	L_Kid.
SAM [22]	86.0±5.5	87.6±8.7	84.5±8.9	53.4±10.6	77.5±16.1	44.5±16.3	19.4±14.0	33.9±15.0	52.4±16.4	35.2±6.8	68.0±11.2	44.4±12.4	82.6±11.3
MedSAM [17]	93.0±3.1	90.0±5.3	89.1±11.0	73.5±9.6	82.5±19.7	76.5±19.4	36.0±23.6	48.7±22.6	56.4±27.1	64.7±19.9	84.0±13.0	53.9±11.7	89.7±7.9
SAM-Med2D [19]	91.4±5.8	83.7±17.3	83.9±15.2	58.8±18.7	60.6±22.5	18.6±10.4	10.6±9.7	27.1±12.4	32.9±21.6	28.1±13.3	72.9±16.6	45.4±19.8	86.0±16.8
SAM-Med3D [40]	85.4±13.2	84.2±9.5	84.7±11.8	46.9±14.3	60.4±10.7	44.5±13.4	32.6±20.9	35.3±18.3	56.0±19.4	32.6±16.4	46.9±19.8	27.4±13.6	84.9±6.9
SegVol [39]	83.9±25.3	71.7±30.6	75.9±28.8	69.4±16.1	83.1±12.1	80.3±13.9	42.1±13.3	49.7±22.6	53.6±31.1	69.6±8.4	81.1±20.7	55.6±19.8	75.1±22.6
CT-SAM3D [41]	95.6±2.0	95.0±1.8	96.1±4.4	83.6±12.0	94.5±2.8	91.8±4.7	78.4±18.0	82.5±4.0	88.4±8.1	82.9±18.1	92.3±4.4	73.2±16.8	94.8±1.4
Universal [†] [13]	97.4±1.4	95.5±6.7	96.4±1.45	73.7±29.6	84.9±10.2	84.4±9.4	72.9±19.5	73.4±14.3	86.0±8.8	76.8±17.4	88.5±16.0	74.5±11.3	96.9±0.8
ZePT [†] [12]	96.7±2.0	95.6±7.7	96.6±2.9	84.3±2.5	90.0±9.0	84.4±2.5	67.2±20.4	66.8±10.1	79.6±9.5	74.2±17.3	85.2±11.1	59.1±11.8	97.2±1.0
CAT	97.7±1.3	96.3±6.1	97.1±1.1	89.2±7.6	90.5±9.1	88.0±2.9	73.6±18.3	74.3±10.0	83.0±10.0	80.1±9.2	88.2±12.3	73.4±8.8	97.3±0.7

Table 7: Segmentation performance of tumors on MSD [59] and In-house dataset. We compare our method with traditional and promptable methods. † denotes obtained via the official pre-trained weights. * means implemented from the official code and trained on the same dataset.

Method	MSD Dataset (Tumor in Abdomen)				In-house Data (Colon Tumor)			
	Liver	Pancreas	Hepatic Vessel	Colon	T1	T2	T3	T4
nnUNet* [62]	66.42±26.5	43.50±34.1	66.90±21.1	41.41±27.8	19.51±33.8	45.06±33.9	44.87±32.4	45.54±29.9
Swin UNETR* [48]	68.67±23.1	41.77±32.9	63.32±25.5	39.35±28.6	21.40±22.2	33.32±30.4	46.11±25.3	52.72±22.8
SAM-Med3D [†] [40]	44.78±38.7	40.05±18.3	44.86±26.3	39.23±19.1	34.28±23.4	42.65±19.1	50.20±16.9	42.65±18.8
SegVol [†] [39]	66.20±26.0	46.36±28.8	68.57±28.2	60.63±24.1	36.93±33.5	42.63±27.8	60.17±27.2	49.83±28.1
Universal [†] [13]	65.68±27.2	45.72±31.9	66.31±21.5	42.26±30.4	7.11±12.3	43.28±29.6	46.52±28.6	53.08±26.9
ZePT [†] [12]	68.58±24.3	44.39±34.2	68.12±20.6	40.38±29.9	23.87±23.8	34.64±32.2	50.81±28.2	51.09±25.5
CAT	72.73±23.3	49.67±32.7	70.11±19.7	48.31±27.3	30.62±31.5	45.61±30.8	55.85±27.7	57.37±23.4

Further results are depicted in Figure 3. Our model demonstrates the capability to segment all structures of the aorta, including the arcus aortae. This comprehensive segmentation is advantageous in real-world scenarios, although it slightly lowers the Dice score.

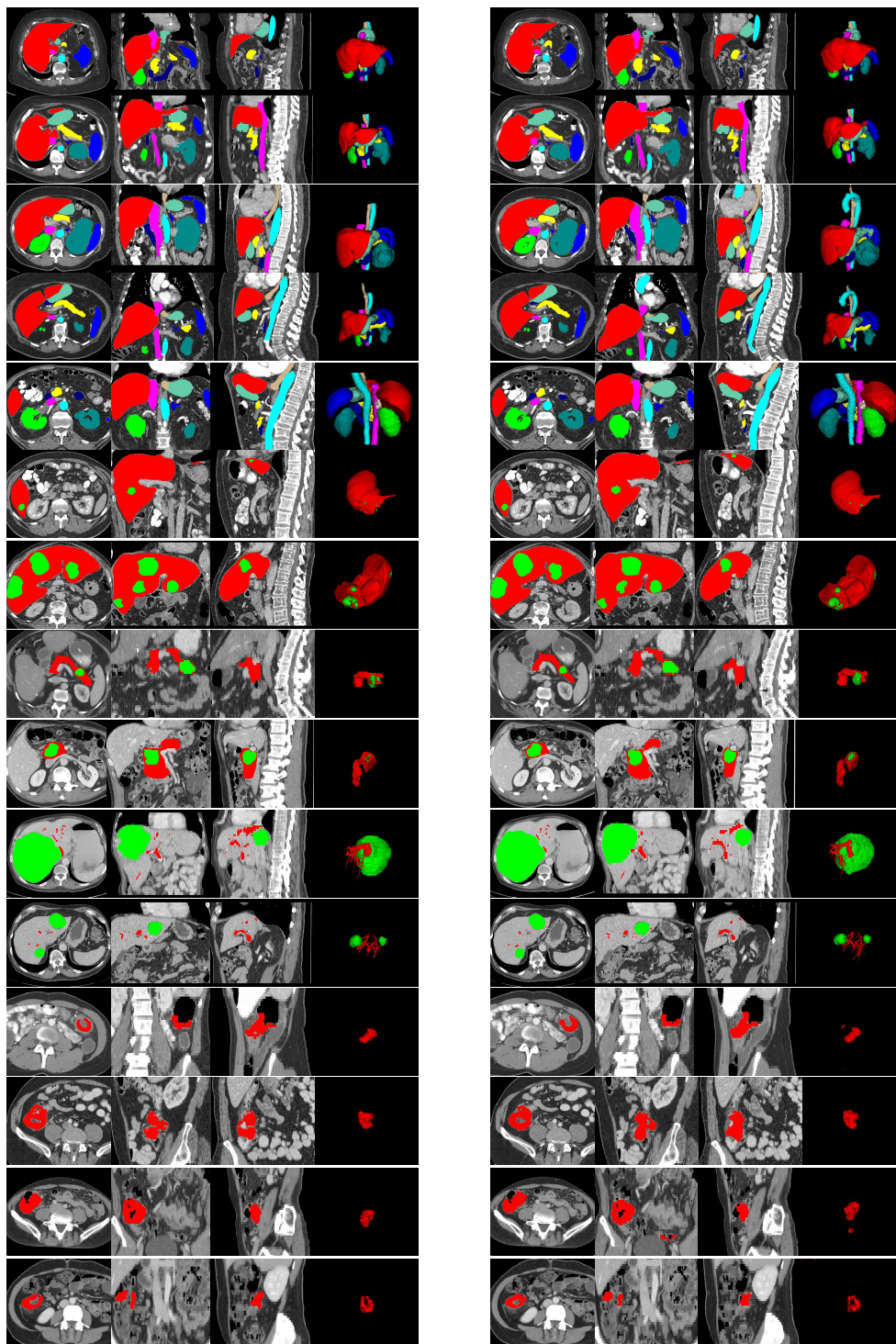


Figure 6: Visualization of segmentation result of *CAT*. The left part is the ground truth and the right part is ours. The first five rows are results of organ segmentation results, and the others are tumor segmentation results. From the top to down are liver tumors, pancreas tumors, Hepatic Vessel tumors, colon tumors, and colon tumors in T4. For each tumor type, we present two cases.

NeurIPS Paper Checklist

1. Claims

Question: Do the main claims made in the abstract and introduction accurately reflect the paper's contributions and scope?

Answer: [\[Yes\]](#)

Justification: The main claims presented in the abstract and introduction of the paper accurately reflect the contributions and scope of the research documented. Both sections clearly articulate the theoretical and experimental advancements achieved, aligning with the results discussed in the subsequent sections of the paper.

Guidelines:

- The answer NA means that the abstract and introduction do not include the claims made in the paper.
- The abstract and/or introduction should clearly state the claims made, including the contributions made in the paper and important assumptions and limitations. A No or NA answer to this question will not be perceived well by the reviewers.
- The claims made should match theoretical and experimental results, and reflect how much the results can be expected to generalize to other settings.
- It is fine to include aspirational goals as motivation as long as it is clear that these goals are not attained by the paper.

2. Limitations

Question: Does the paper discuss the limitations of the work performed by the authors?

Answer: [\[Yes\]](#)

Justification: The paper discusses the limitations in Section 5.

Guidelines:

- The answer NA means that the paper has no limitation while the answer No means that the paper has limitations, but those are not discussed in the paper.
- The authors are encouraged to create a separate "Limitations" section in their paper.
- The paper should point out any strong assumptions and how robust the results are to violations of these assumptions (e.g., independence assumptions, noiseless settings, model well-specification, asymptotic approximations only holding locally). The authors should reflect on how these assumptions might be violated in practice and what the implications would be.
- The authors should reflect on the scope of the claims made, e.g., if the approach was only tested on a few datasets or with a few runs. In general, empirical results often depend on implicit assumptions, which should be articulated.
- The authors should reflect on the factors that influence the performance of the approach. For example, a facial recognition algorithm may perform poorly when image resolution is low or images are taken in low lighting. Or a speech-to-text system might not be used reliably to provide closed captions for online lectures because it fails to handle technical jargon.
- The authors should discuss the computational efficiency of the proposed algorithms and how they scale with dataset size.
- If applicable, the authors should discuss possible limitations of their approach to address problems of privacy and fairness.
- While the authors might fear that complete honesty about limitations might be used by reviewers as grounds for rejection, a worse outcome might be that reviewers discover limitations that aren't acknowledged in the paper. The authors should use their best judgment and recognize that individual actions in favor of transparency play an important role in developing norms that preserve the integrity of the community. Reviewers will be specifically instructed to not penalize honesty concerning limitations.

3. Theory Assumptions and Proofs

Question: For each theoretical result, does the paper provide the full set of assumptions and a complete (and correct) proof?

Answer: [\[NA\]](#)

Justification: Our paper is based on solid experimental results and does not involve theoretical outcomes.

Guidelines:

- The answer NA means that the paper does not include theoretical results.

- All the theorems, formulas, and proofs in the paper should be numbered and cross-referenced.
- All assumptions should be clearly stated or referenced in the statement of any theorems.
- The proofs can either appear in the main paper or the supplemental material, but if they appear in the supplemental material, the authors are encouraged to provide a short proof sketch to provide intuition.
- Inversely, any informal proof provided in the core of the paper should be complemented by formal proofs provided in appendix or supplemental material.
- Theorems and Lemmas that the proof relies upon should be properly referenced.

4. **Experimental Result Reproducibility**

Question: Does the paper fully disclose all the information needed to reproduce the main experimental results of the paper to the extent that it affects the main claims and/or conclusions of the paper (regardless of whether the code and data are provided or not)?

Answer: [Yes]

Justification: The information needed to reproduce the main experimental results is introduced in Section 3 and Section 4.

Guidelines:

- The answer NA means that the paper does not include experiments.
- If the paper includes experiments, a No answer to this question will not be perceived well by the reviewers: Making the paper reproducible is important, regardless of whether the code and data are provided or not.
- If the contribution is a dataset and/or model, the authors should describe the steps taken to make their results reproducible or verifiable.
- Depending on the contribution, reproducibility can be accomplished in various ways. For example, if the contribution is a novel architecture, describing the architecture fully might suffice, or if the contribution is a specific model and empirical evaluation, it may be necessary to either make it possible for others to replicate the model with the same dataset, or provide access to the model. In general, releasing code and data is often one good way to accomplish this, but reproducibility can also be provided via detailed instructions for how to replicate the results, access to a hosted model (e.g., in the case of a large language model), releasing of a model checkpoint, or other means that are appropriate to the research performed.
- While NeurIPS does not require releasing code, the conference does require all submissions to provide some reasonable avenue for reproducibility, which may depend on the nature of the contribution. For example
 - (a) If the contribution is primarily a new algorithm, the paper should make it clear how to reproduce that algorithm.
 - (b) If the contribution is primarily a new model architecture, the paper should describe the architecture clearly and fully.
 - (c) If the contribution is a new model (e.g., a large language model), then there should either be a way to access this model for reproducing the results or a way to reproduce the model (e.g., with an open-source dataset or instructions for how to construct the dataset).
 - (d) We recognize that reproducibility may be tricky in some cases, in which case authors are welcome to describe the particular way they provide for reproducibility. In the case of closed-source models, it may be that access to the model is limited in some way (e.g., to registered users), but it should be possible for other researchers to have some path to reproducing or verifying the results.

5. **Open access to data and code**

Question: Does the paper provide open access to the data and code, with sufficient instructions to faithfully reproduce the main experimental results, as described in supplemental material?

Answer: [Yes]

Justification: Codes and data are available at supplemental materials.

Guidelines:

- The answer NA means that paper does not include experiments requiring code.
- Please see the NeurIPS code and data submission guidelines (<https://nips.cc/public/guides/CodeSubmissionPolicy>) for more details.

- While we encourage the release of code and data, we understand that this might not be possible, so “No” is an acceptable answer. Papers cannot be rejected simply for not including code, unless this is central to the contribution (e.g., for a new open-source benchmark).
- The instructions should contain the exact command and environment needed to run to reproduce the results. See the NeurIPS code and data submission guidelines (<https://nips.cc/public/guides/CodeSubmissionPolicy>) for more details.
- The authors should provide instructions on data access and preparation, including how to access the raw data, preprocessed data, intermediate data, and generated data, etc.
- The authors should provide scripts to reproduce all experimental results for the new proposed method and baselines. If only a subset of experiments are reproducible, they should state which ones are omitted from the script and why.
- At submission time, to preserve anonymity, the authors should release anonymized versions (if applicable).
- Providing as much information as possible in supplemental material (appended to the paper) is recommended, but including URLs to data and code is permitted.

6. Experimental Setting/Details

Question: Does the paper specify all the training and test details (e.g., data splits, hyper-parameters, how they were chosen, type of optimizer, etc.) necessary to understand the results?

Answer: [Yes]

Justification: All the training and test details can be seen in Section 4 and Appendix A.2 A.3. Guidelines:

- The answer NA means that the paper does not include experiments.
- The experimental setting should be presented in the core of the paper to a level of detail that is necessary to appreciate the results and make sense of them.
- The full details can be provided either with the code, in appendix, or as supplemental material.

7. Experiment Statistical Significance

Question: Does the paper report error bars suitably and correctly defined or other appropriate information about the statistical significance of the experiments?

Answer: [Yes]

Justification: The paper reports the Standard Deviation in Table 6 and Table 7.

Guidelines:

- The answer NA means that the paper does not include experiments.
- The authors should answer "Yes" if the results are accompanied by error bars, confidence intervals, or statistical significance tests, at least for the experiments that support the main claims of the paper.
- The factors of variability that the error bars are capturing should be clearly stated (for example, train/test split, initialization, random drawing of some parameter, or overall run with given experimental conditions).
- The method for calculating the error bars should be explained (closed form formula, call to a library function, bootstrap, etc.)
- The assumptions made should be given (e.g., Normally distributed errors).
- It should be clear whether the error bar is the standard deviation or the standard error of the mean.
- It is OK to report 1-sigma error bars, but one should state it. The authors should preferably report a 2-sigma error bar than state that they have a 96% CI, if the hypothesis of Normality of errors is not verified.
- For asymmetric distributions, the authors should be careful not to show in tables or figures symmetric error bars that would yield results that are out of range (e.g. negative error rates).
- If error bars are reported in tables or plots, The authors should explain in the text how they were calculated and reference the corresponding figures or tables in the text.

8. Experiments Compute Resources

Question: For each experiment, does the paper provide sufficient information on the computer resources (type of compute workers, memory, time of execution) needed to reproduce the experiments?

Answer: [Yes]

Justification: Sufficient information on the computer resources can be seen in Section A.3.
Guidelines:

- The answer NA means that the paper does not include experiments.
- The paper should indicate the type of compute workers CPU or GPU, internal cluster, or cloud provider, including relevant memory and storage.
- The paper should provide the amount of compute required for each of the individual experimental runs as well as estimate the total compute.
- The paper should disclose whether the full research project required more compute than the experiments reported in the paper (e.g., preliminary or failed experiments that didn't make it into the paper).

9. Code Of Ethics

Question: Does the research conducted in the paper conform, in every respect, with the NeurIPS Code of Ethics <https://neurips.cc/public/EthicsGuidelines>?

Answer: [Yes]

Justification: Authors have reviewed the NeurIPS Code of Ethics.

Guidelines:

- The answer NA means that the authors have not reviewed the NeurIPS Code of Ethics.
- If the authors answer No, they should explain the special circumstances that require a deviation from the Code of Ethics.
- The authors should make sure to preserve anonymity (e.g., if there is a special consideration due to laws or regulations in their jurisdiction).

10. Broader Impacts

Question: Does the paper discuss both potential positive societal impacts and negative societal impacts of the work performed?

Answer: [Yes]

Justification: The paper discusses both the potential positive societal impacts and negative societal impacts of the work in Section 5.

Guidelines:

- The answer NA means that there is no societal impact of the work performed.
- If the authors answer NA or No, they should explain why their work has no societal impact or why the paper does not address societal impact.
- Examples of negative societal impacts include potential malicious or unintended uses (e.g., disinformation, generating fake profiles, surveillance), fairness considerations (e.g., deployment of technologies that could make decisions that unfairly impact specific groups), privacy considerations, and security considerations.
- The conference expects that many papers will be foundational research and not tied to particular applications, let alone deployments. However, if there is a direct path to any negative applications, the authors should point it out. For example, it is legitimate to point out that an improvement in the quality of generative models could be used to generate deepfakes for disinformation. On the other hand, it is not needed to point out that a generic algorithm for optimizing neural networks could enable people to train models that generate Deepfakes faster.
- The authors should consider possible harms that could arise when the technology is being used as intended and functioning correctly, harms that could arise when the technology is being used as intended but gives incorrect results, and harms following from (intentional or unintentional) misuse of the technology.
- If there are negative societal impacts, the authors could also discuss possible mitigation strategies (e.g., gated release of models, providing defenses in addition to attacks, mechanisms for monitoring misuse, mechanisms to monitor how a system learns from feedback over time, improving the efficiency and accessibility of ML).

11. Safeguards

Question: Does the paper describe safeguards that have been put in place for responsible release of data or models that have a high risk for misuse (e.g., pretrained language models, image generators, or scraped datasets)?

Answer: [NA]

Justification: Our paper poses no such risks.

Guidelines:

- The answer NA means that the paper poses no such risks.

- Released models that have a high risk for misuse or dual-use should be released with necessary safeguards to allow for controlled use of the model, for example by requiring that users adhere to usage guidelines or restrictions to access the model or implementing safety filters.
- Datasets that have been scraped from the Internet could pose safety risks. The authors should describe how they avoided releasing unsafe images.
- We recognize that providing effective safeguards is challenging, and many papers do not require this, but we encourage authors to take this into account and make a best faith effort.

12. Licenses for existing assets

Question: Are the creators or original owners of assets (e.g., code, data, models), used in the paper, properly credited and are the license and terms of use explicitly mentioned and properly respected?

Answer: [\[Yes\]](#)

Justification: We cite the original paper that produced the code package or dataset.

Guidelines:

- The answer NA means that the paper does not use existing assets.
- The authors should cite the original paper that produced the code package or dataset.
- The authors should state which version of the asset is used and, if possible, include a URL.
- The name of the license (e.g., CC-BY 4.0) should be included for each asset.
- For scraped data from a particular source (e.g., website), the copyright and terms of service of that source should be provided.
- If assets are released, the license, copyright information, and terms of use in the package should be provided. For popular datasets, paperswithcode.com/datasets has curated licenses for some datasets. Their licensing guide can help determine the license of a dataset.
- For existing datasets that are re-packaged, both the original license and the license of the derived asset (if it has changed) should be provided.
- If this information is not available online, the authors are encouraged to reach out to the asset's creators.

13. New Assets

Question: Are new assets introduced in the paper well documented and is the documentation provided alongside the assets?

Answer: [\[NA\]](#)

Justification: The paper does not release new assets.

Guidelines:

- The answer NA means that the paper does not release new assets.
- Researchers should communicate the details of the dataset/code/model as part of their submissions via structured templates. This includes details about training, license, limitations, etc.
- The paper should discuss whether and how consent was obtained from people whose asset is used.
- At submission time, remember to anonymize your assets (if applicable). You can either create an anonymized URL or include an anonymized zip file.

14. Crowdsourcing and Research with Human Subjects

Question: For crowdsourcing experiments and research with human subjects, does the paper include the full text of instructions given to participants and screenshots, if applicable, as well as details about compensation (if any)?

Answer: [\[NA\]](#)

Justification: The paper does not involve crowdsourcing or research with human subjects.

Guidelines:

- The answer NA means that the paper does not involve crowdsourcing nor research with human subjects.
- Including this information in the supplemental material is fine, but if the main contribution of the paper involves human subjects, then as much detail as possible should be included in the main paper.

- According to the NeurIPS Code of Ethics, workers involved in data collection, curation, or other labor should be paid at least the minimum wage in the country of the data collector.

15. Institutional Review Board (IRB) Approvals or Equivalent for Research with Human Subjects

Question: Does the paper describe potential risks incurred by study participants, whether such risks were disclosed to the subjects, and whether Institutional Review Board (IRB) approvals (or an equivalent approval/review based on the requirements of your country or institution) were obtained?

Answer: [\[Yes\]](#)

Justification: We obtain Institutional Review Board approvals of the in-house dataset and there is no potential risks.

Guidelines:

- The answer NA means that the paper does not involve crowdsourcing nor research with human subjects.
- Depending on the country in which research is conducted, IRB approval (or equivalent) may be required for any human subjects research. If you obtained IRB approval, you should clearly state this in the paper.
- We recognize that the procedures for this may vary significantly between institutions and locations, and we expect authors to adhere to the NeurIPS Code of Ethics and the guidelines for their institution.
- For initial submissions, do not include any information that would break anonymity (if applicable), such as the institution conducting the review.